Journal of Alzheimer's Disease 99 (2024) 223–240
DOI 10.3233/JAD-231182
IOS Press

Multi-Ethnic Norms for Volumes of Subcortical and Lobar Brain Structures Measured by Neuro I: Ethnicity May Improve the Diagnosis of Alzheimer's Disease[1]

Yu Yong Choi[a,b], Jang Jae Lee[a], Jan te Nijenhuis[a], Kyu Yeong Choi[a], Jongseong Park[c], Jongmyoung Ok[c], IL Han Choo[d], Hoowon Kim[a,e], Min-Kyung Song[b], Seong-Min Choi[b,f], Soo Hyun Cho[b,f], Youngshik Choe[g], Byeong C. Kim[b,f,*] and Kun Ho Lee[a,c,g,h,*]

[a]*Gwangju Alzheimer's & Related Dementia Cohort Research Center, Chosun University, Gwangju, Republic of Korea*
[b]*Department of Neurology, Chonnam National University Hospital, Gwangju, Republic of Korea*
[c]*Neurozen Inc., Seoul, Republic of Korea*
[d]*Department of Neuropsychiatry, Chosun University School of Medicine and Hospital, Gwangju, Republic of Korea*
[e]*Department of Neurology, Chosun University School of Medicine and Hospital, Gwangju, Republic of Korea*
[f]*Department of Neurology, Chonnam National University Medical School, Gwangju, Republic of Korea*
[g]*Korea Brain Research Institute, Daegu, Republic of Korea*
[h]*Department of Biomedical Science, Chosun University, Gwangju, Republic of Korea*

Accepted 28 February 2024
Pre-press 16 April 2024

Abstract.
Background: We previously demonstrated the validity of a regression model that included ethnicity as a novel predictor for predicting normative brain volumes in old age. The model was optimized using brain volumes measured with a standard tool FreeSurfer.
Objective: Here we further verified the prediction model using newly estimated brain volumes from Neuro I, a quantitative brain analysis system developed for Korean populations.
Methods: Lobar and subcortical volumes were estimated from MRI images of 1,629 normal Korean and 786 Caucasian subjects (age range 59–89) and were predicted in linear regression from ethnicity, age, sex, intracranial volume, magnetic field strength, and scanner manufacturers.

[1]Some of the Caucasian data were from the ADNI project launched in 2003 as a public-private partnership, led by Principal Investigator Michael W. Weiner (see http://www.adni-info.org/ for up-to-date information).

*Correspondence to: Byeong C. Kim, Department of Neurology, Chonnam National University Hospital, Gwangju 61469, Republic of Korea. E-mail: byeong.kim7@gmail.com and Kun Ho Lee, a Gwangju Alzheimer's & Related Dementia Cohort Research Center, Chosun University, Gwangju 61452, Republic of Korea. E-mail: leekho@chosun.ac.kr.

Results: In the regression model predicting the new volumes, ethnicity was again a substantial predictor in most regions. Additionally, the model-based z-scores of regions were calculated for 428 AD patients and the matched controls, and then employed for diagnostic classification. When the AD classifier adopted the z-scores adjusted for ethnicity, the diagnostic accuracy has noticeably improved (AUC = 0.85, ΔAUC = + 0.04, $D = 4.10$, $p < 0.001$).

Conclusions: Our results suggest that the prediction model remains robust across different measurement tool, and ethnicity significantly contributes to the establishment of norms for brain volumes and the development of a diagnostic system for neurodegenerative diseases.

Keywords: Alzheimer's disease, brain aging, ethnic difference, magnetic resonance imaging, norm

INTRODUCTION

Normative values for brain structures are needed when calculating an individual's brain volume alternation, so that we can determine the degree of brain diseases, or deviation from the norm, in light of that individual's characteristics. Starting two decades ago, there had only been few attempts to establish norms [1, 2] because collecting sufficient brain images of healthy individuals is laborious and expensive. A decade ago, a notable series of studies was conducted [3, 4] in which a large number of images from multiple MRI studies were integrated, and physical and technical features of different MRI scanners were considered; moreover, at the level of individuals, there was also attention for demographical background and anatomy [5], allowing the establishment of norms for brain volumes.

Recent research has shown ethnicity to be an essential factor in the establishment of brain norms [6]. Although it was already known that there are racial differences in brain morphometry [7–10], this did not lead to establishing brain norms in Western societies that also included racial minorities [11–14]. Particularly, there is a growing need for specialized norms for the elderly covering Asians as well as Caucasians. In 2020, Asians comprised 56.7% of the world's elderly population, or 414 million people; by 2060, the number is projected to nearly triple to 1,216 million, which is 61.5% of the world total [15]. Moreover, as Choi, et al. [6] mentioned, the establishment of norms unique to a restricted age range has benefits. First, the norm model could be simple and non-overfitted because volume and age most likely are linearly related, and second, the model would provide more accurate and reliable estimates with the same number of samples.

In a previous study, we validated a regression model for predicting normative brain volumes of a healthy individual in old age based on their ethnicity and raw volumes obtained through a standard tool, FreeSurfer [6]. Here we further validated the prediction models. In this study, instead of FreeSurfer we used Neuro I, which is a neuroimaging quantitative analysis system developed to provide brain volumes and norms suitable for Korean population. We utilized the fresh volume measurement to acquire lobar and subcortical volumes from extensive collections of MRI images taken from healthy elderly individuals of Korean and Caucasian origins, which were subsequently examined within our predictive model.

MATERIALS AND METHODS

We note that our method section builds strongly upon the method section described in Choi et al. [6].

The studies involving human participants were approved by the Institutional Review Board of Chosun University Hospital, Gwangju, Republic of Korea. All volunteers or the next of kin of patients gave written informed consent before participation.

Measurement of cortical and subcortical volumes

To measure the volumes of cortical and subcortical structures, we processed T1 brain images of all subjects using Neuro I (version 1.3; for detailed information, see http://neurozen.ai/) which is a commercial software package for quantitative neuroimaging analysis. Figure 1 depicted the procedure that consisted of the following steps. 1) T1 images were corrected for bias field inhomogeneity through the self-developed software component based on the N4 algorithm [16]. 2) The corrected images were skull-stripped using the three-dimensional convolutional neural network (3D CNN) deep learning models for intracranial volume (ICV) and brain delimitation [17, 18]. 3) The preprocessed images underwent segmentation into 107 regions of interest (ROIs) of the Desikan-Killiany-Tourville (DKT) atlas by using a 3D CNN model for brain regional parcellation. Then, cortical volumes were calculated

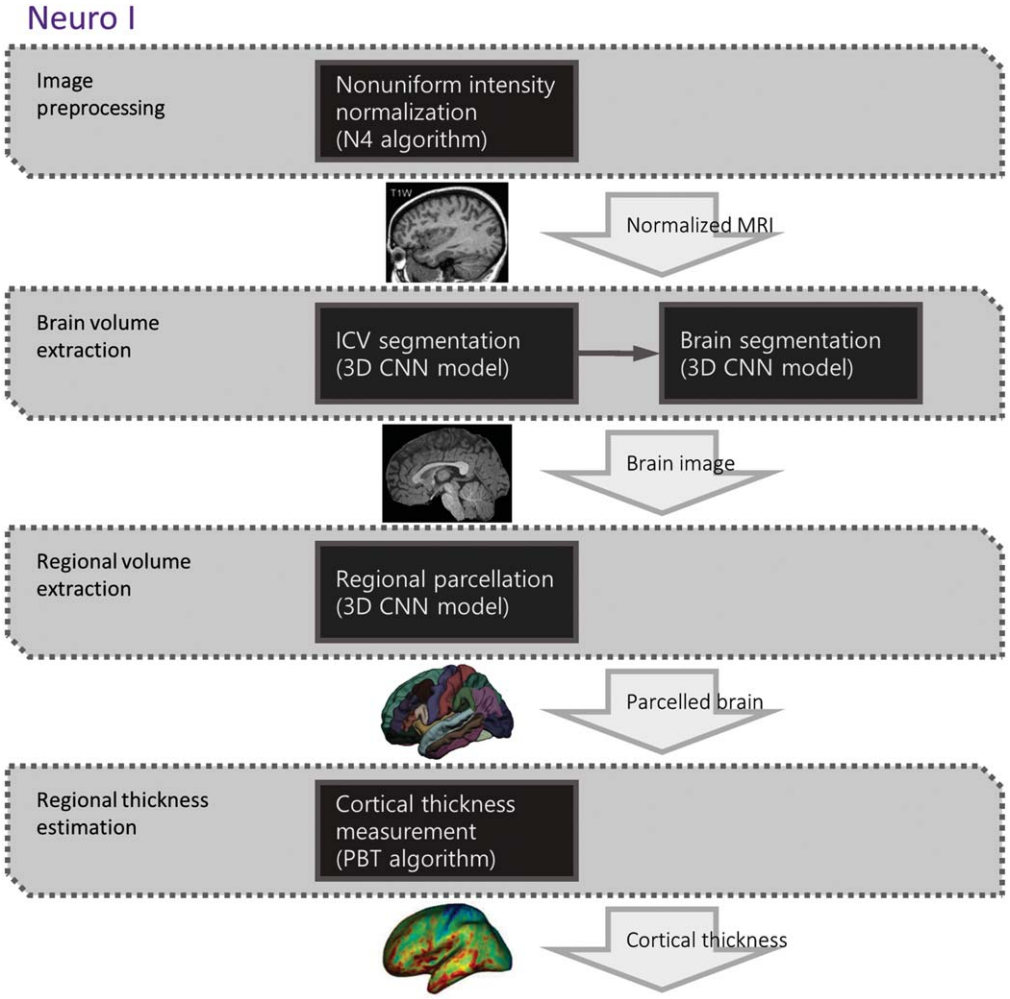

Fig. 1. Data processing procedure for brain volume and cortical thickness measurement in Neuro I. ICV, intracranial volume; CNN, convolutional neural network; PBT, projection-based thickness.

by counting voxel numbers in each ROI. 4) Cortical thickness of each ROI was estimated by using the self-developed software component based on a projection-based thickness (PBT) algorithm [19]. We note that cortical thickness was not analyzed in this paper.

As part of the quality control for image data processing result, the final step in Fig. 2 involved examining ICV values, which significantly impact the norm model. This examination led to the exclusion of data associated with ICV values identified as outliers. Additionally, a new step introduced in this paper checks whether the difference in ICV values between FreeSurfer and Neuro I (calculated as $2(ICV_{FreeSurfer} - ICV_{Neuro\ I})/(ICV_{FreeSurfer} + ICV_{Neuro\ I})$) qualifies as an outlier. This new step resulted in a minor reduction in the sample size compared to our previous paper [6].

Normative samples for Koreans

As described in Choi et al. [6], all the participants were enrolled in the Gwangju Alzheimer's and Related Dementia (GARD) cohort of the GARD Cohort Research Center located in Gwangju, Republic of Korea, between April 2010 and March 2018. All the participants underwent a thorough evaluation, which included comprehensive interviews, neurological examinations, and neuropsychological tests. The neuropsychological tests consisted of the Korean version of the Mini-Mental State Examination (K-MMSE) [20], and the Seoul Neuropsychological

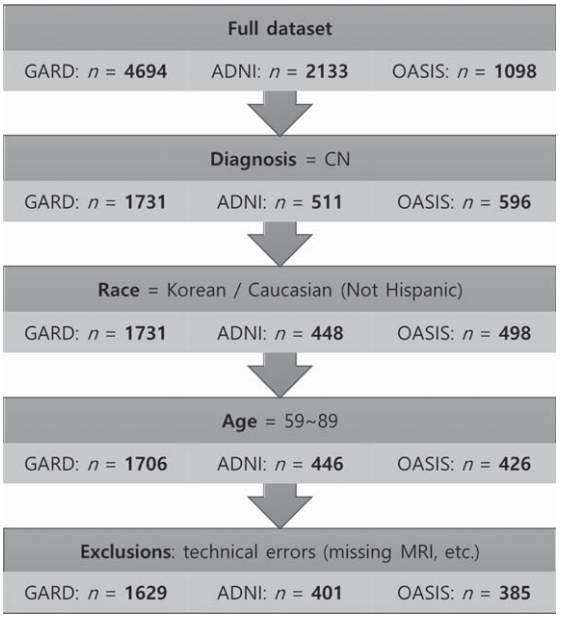

Fig. 2. Flowchart of the process of subject selection for the norms. The normative sample finally comprised 2,415 subjects: 1,629 for Koreans and 786 for Caucasians. CN, cognitively normal; GARD, Gwangju Alzheimer's & Related Dementia; ADNI, Alzheimer's Disease Neuroimaging Initiative; OASIS, Open Access Series of Imaging Studies.

Screening Battery (SNSB) [21]. Additionally, the Clinical Dementia Rating [22] was administered. To be eligible for inclusion in the study, participants were required to satisfy specific conditions, which encompassed the absence of a focal brain lesion, no prior head trauma history, and the absence of psychiatric disorders potentially impacting their cognitive abilities. Minor medical irregularities were not grounds for exclusion [6].

Normative samples for Caucasians

To investigate ethnic differences, we collected data from the Alzheimer's Disease Neuroimaging Initiative (ADNI) and the Open Access Series of Imaging Studies (OASIS) databases on Caucasians (851 CN cases), excluding Hispanic subjects (cf. http://adni.loni.usc.edu and https://www.oasis-brains.org).

The ADNI database supplied a part of the Caucasian data on which this paper was based. ADNI was mainly set up to test whether various biological markers, and various assessments can be combined to measure how mild cognitive impairment and early Alzheimer's disease (AD) progress. The ADNI website (http://www.adni-info.org) supplies the latest material.

MRI acquisition

Korean participants underwent brain scans using a 3.0 T MRI scanner (Siemens Skyra) equipped with a 20-channel head coil and a 1.5 T MRI scanner (Siemens Avanto) with a 12-channel head coil. The scans included MPRAGE sagittal views and MPRAGE axial views. The MRI protocol for Koreans was described in detail in Choi, et al. [6]. For Caucasians, brain scans were conducted using 3.0 T and 1.5 T MRI scanners across various centers for ADNI, and a 3.0 T scanner for OASIS. The protocols for Caucasians can be found on the ADNI and the OASIS sites (cf. https://adni.loni.usc.edu/methods/documents/mri-protocols/ and https://www.oasis-brains.org/files/OASIS-3_Imaging_Data_Dictionary_v2.0.pdf).

Statistical analyses

We performed the statistical analyses identically as in our previous study where we used R (version 4.2.0, available at https://www.r-project.org/). In the regression model analyses we used five predictors: age, sex, intracranial volume (ICV), magnetic field strength (MFS), and scanner manufacturers [6]. The initial model prior to incorporating ethnicity as a predictor was structured as follows:

$$\hat{V} = \beta_1 \cdot age + \beta_2 \cdot sex + \beta_3 \cdot ICV + \beta_4 \cdot ICV^2 + \beta_5 \cdot ICV^3 + \beta_6 \cdot MFS + \beta_7 \cdot manufacturer + \beta_8 \cdot sex \times age + \beta_9 \cdot MFS \times manufacturer + \beta_{10} \cdot MFS \times ICV + \beta_{11} \cdot ICV \times manufacturer + \alpha$$

The ultimate model, incorporating ethnicity and the interaction terms *ethnicity* × *age* and *ethnicity* × *sex*, was structured as follows:

$$\hat{V} = \beta_1 \cdot \boldsymbol{ethnicity} + \beta_2 \cdot \boldsymbol{ethnicity} \times \boldsymbol{age} + \beta_3 \cdot \boldsymbol{ethnicity} \times \boldsymbol{sex} + \beta_4 \cdot age + \beta_5 \cdot sex + \beta_6 \cdot ICV + \beta_7 \cdot ICV^2 + \beta_8 \cdot ICV^3 + \beta_9 \cdot MFS + \beta_{10} \cdot manufacturer + \beta_{11} \cdot sex \times age + \beta_{12} \cdot MFS \times manufacturer + \beta_{13} \cdot MFS \times ICV + \beta_{14} \cdot ICV \times manufacturer + \alpha$$

We conducted ten-fold cross-validation on all the predictive models utilizing the caret package to avoid overfitting and enhance generalizability. Due to the non-normal distribution of ventricular volumes, we applied a logarithmic transformation to them, and the resulting coefficients were adjusted to represent cm^3 or % increase per year for better readability.

The z-score distributions for the four groups, which include AD patients and normal controls from both Koreans and Caucasians, were established following inter-group matching that considered age, sex, and MFS. A propensity score matching technique from the MatchIt package was used in the selection process of normal controls to match with AD patients from the normative samples previously mentioned. The details of the four groups can be found in Table 4.

Normative statistics

We calculated the discrepancies between a given subject's obtained volume (V_0) and the volume predicted by the regression model ($\hat{V}$) following the approach given by Crawford et al. [23].

The initial stage involves the computation of the standard error (SE) for a projected volume of a new individual, referred to as s_{n+1}. The SE can be represented using the following formula:

$$s_{n+1} = s_{V \cdot x} \cdot \sqrt{1 + \frac{1}{n} + \frac{1}{n-1}\sum r^{ii} z_{i0}^2 + \frac{2}{n-1}\sum r^{ij} z_{i0} z_{j0}}$$

Here, $s_{V \cdot x}$ signifies the standard error of estimate or root mean square error of the model predicting normative values. The term r^{ii} denotes the elements on the main diagonal of the inverted correlation matrix (R^{-1}) for the k predictor variables, while r^{ij} refers to the off-diagonal elements. Additionally, and $z_0 = (z_{10}, \ldots, z_{k0})'$ represents the subject's values on the predictor variables in z-score form. The calculation of z_{i0} is based on the formula $z_{i0} = (n-1)(x_{i0} - \bar{x}_i) / \Sigma(x_{ij} - \bar{x}_i)^2$. The first summation pertains to the k diagonal elements, and the second summation covers the $k(k\text{-}1)/2$ off-diagonal elements either below or above the diagonal. To estimate the effect size, we computed a z-score (z) using the formula:

$$z = \frac{V_0 - \hat{V}}{s_{n+1}}$$

The equation represents the discrepancy between a subject's actual (V_0) and predicted volumes ($\hat{V}$), divided by the standard error of the predicted volume (s_{n+1}).

Diagnosing Koreans with AD from Caucasian controls

Logistic regression models with/without ethnicity as a predictor were constructed based on the z-scores from six ROIs, specifically the amygdala, hippocampus, and temporal lobe in both left and right hemispheres. The optimal classification model was identified through a 10-fold cross-validation, and the two receiver operating curves (ROCs) and their respective areas under the ROC (AUCs) were computed. To obtain a reliable estimate of population parameters, the significance of AUC comparisons was assessed using non-parametric stratified resampling [24] with 10,000 bootstrap replications. The caret and the pROC packages were employed for the analysis.

RESULTS

Subject selection and demographic information

The normative sample for this study, consisting of 2,415 subjects, was selected based on the inclusion and exclusion criteria outlined in Fig. 2 [6]. All subjects in the normative sample were selected from the cohort classified as cognitively normal (CN). The sample was comprised of 1629 Korean subjects from the GARD cohort and 786 Caucasian subjects from the ADNI and the OASIS datasets. The age range of the Caucasian subjects matched that of the Korean sample, which was 59 to 89 years old. Demographic information for the normative sample is provided in Table 1.

Predictive model that incorporates ethnicity as a predictor to forecast a brain volume

Fit measures and standardized coefficients of the models predicting subcortical and cortical volumes of the Korean and Caucasian normal controls ($n = 2415$) can be found in Table 2. The models aimed at predicting subcortical gray matter volumes accounted for significant portions of the variance (R^2: mean = 44.4%, range = 28.4–59.9%). Moreover, the models targeting lobar gray matter volumes explained even great extent of variance (R^2: mean = 62.4%, range = 42.6–77.3%). Table 2 shows that ethnicity had a notable impact on most regions, whereas age

Table 1
Cohort sizes and demographics for normal Koreans and Caucasians

Race	Dataset	n	F	3T	Age (y)			MMSE		Education (y)	
					range	*M*	±*SD*	*M*	±*SD*	*M*	±*SD*
Korean	GARD	1629	63%	82%	59–89	73.0	±5.5	27.0	±2.1	9.6	±4.6
Caucasian	ADNI, OASIS	786	54%	77%	59–89	73.3	±6.2	29.2	±1.1	16.3	±2.6

GARD, Gwangju Alzheimer's & Related Dementia; ADNI, Alzheimer's Disease Neuroimaging Initiative; OASIS, Open Access Series of Imaging Studies. F, female; y, years; MMSE, Mini-Mental State Examination.

exerted a considerable influence across all regions except the left caudate.

Figure 3 and Table 3 show the variance explained by each predictor, indicating its relative importance. Age explained substantial proportions of variance for lobar and subcortical volumes (R^2: mean = 2.8%, 3.0%; range = 1.1–4.8%, 0.1–6.2%, respectively). Ethnicity explained somewhat less but still non-negligible proportions for lobar and subcortical volumes (R^2: mean = 2.1%, 1.3%; range = 0.2–6.9%, 0.2–3.6%, respectively). The ethnicity-relevant terms, including *ethnicity*×*age* and *ethnicity*×*sex* as well as ethnicity, collectively accounted for substantial portions of variance in lobar and subcortical volumes (R^2: mean = 4.0%, 3.3%; range = 1.9–9.1%, 1.7–5.1%).

Table 2 shows that age had a substantial effect on all lobar and subcortical regions except the left caudate, and ethnicity also had a substantial effect on half or more of all the regions such as temporal, parietal, right occipital, left cingulate, and right insular lobes and most of the subcortical regions such as thalami, putamina, hippocampi, caudates, amygdalae, pallidi and left accumbens. Koreans generally had larger lobar and subcortical regions than Caucasians ($\beta<0$, $p<0.00125$), with the left cingulate cortex being the only exception, as it was clearly smaller in Koreans ($\beta>0$, $p<0.00125$).

Alternation in the volume of subcortical and lobar regions during normal aging

Figures 4 and 5 show the rate of aging in brain regions among individuals aged 59 to 89, comparing Caucasians and Koreans. The aging slopes indicated the projected volume changes in the subcortical and lobar regions based on age and ethnicity. In general, there were no significant differences in the aging rates between Koreans and Caucasians. However, as indicated in Table 2, a notable age-by-ethnicity interaction was observed in the insular cortices, left thalamus, right pallidus, and right accumbens ($p<0.00125$). Additionally, a relatively weaker age-by-ethnicity interaction was detected in some regions ($p<0.05$).

Z-scoring before/after accounting for ethnicity

To validate the z-score generated by our predictive model accounting for ethnicity, Korean and Caucasian individuals with AD were additionally collected and their controls were matched. As shown in Table 4, the two racial groups with the two diagnostic categories ($n = 214$ for each group) were well-matched in terms of age, gender, and MFS.

First, we calculated the z-scores for the normal control groups within both Koreans and Caucasians and assessed the statistical significance of the values. Because the z-score reflects the disparities between the observed and predicted volume measurements, the z-scores of the normal controls should be closely approximated zero. As detailed in Table 5, following the ethnicity adjustment, the z-scores for normal controls were no longer statistically significant for both the racial categories, despite their earlier significance in the parietal ($z = -0.60 - 0.56, p<0.00125$), temporal lobes, thalami, right hippocampus, and right accumbens ($z = -0.48$–0.19, $p<0.05$) for either racial category prior to the ethnicity adjustment. Following this ethnicity adjustment, the z-scores for lobar volumes closely approached zero (z in Koreans: mean = 0.03, range = –0.03–0.12; z in Caucasians: mean = 0.04, range = –0.09–0.03), and the z-scores for subcortical volumes similarly converged near zero (z in Koreans: mean = 0.04, range = –0.04–0.11; z in Caucasians: mean = –0.02, range = –0.11–0.08).

Diagnosing Koreans with AD from Caucasian controls

We assessed the effectiveness of our z-scoring method in the AD diagnostic process in a multiracial environment. As shown in Table 6, the z-scores were compared between all combinations of the AD and the control groups of both the races. The distributions of six representative regions were illustrated in Fig. 6. The condition for selecting the representative regions

Table 2
Standardized coefficients of the prediction model of lobar and subcortical gray matter volumes

	MODEL:						COEFFICIENT:			Intracrainial volume			Scanner			Interaction							
	RMSE		R^2		MAE		Age	Ethnicity	Sex	ICV	ICV^2	ICV^3	MFS	Manufacturer		Ethnicity *Age	Ethnicity *Sex	Sex *Age	MFS *GE	MFS* Philips	MFS *ICV	ICV *GE	ICV* Philips
													1.5T/ 3.0T	GE/ Siemens	Philips/ Siemens								
	M	SD	M	SD	M	SD		Cau/Kor	M/F														
brain	27.39	1.45	0.91	0.01	21.35	1.04	***–0.21***	***–0.04***	*–0.10*	***1.02***	0.00	–0.02	***0.06***	***–0.05***	***0.04***	0.01	0.00	**–0.02**	0.02	***–0.05***	0.00	0.00	0.00
lobar gray matter	14.44	0.67	0.85	0.02	11.38	0.53	***–0.22***	***–0.12***	*–0.11*	***0.96***	0.00	–0.02	***–0.05***	***–0.05***	***0.04***	0.01	0.01	–0.02	–0.02	***–0.08***	0.01	–0.01	0.00
frontal L	3.32	0.16	0.74	0.03	2.65	0.12	***–0.17***	–0.01	*–0.10*	***0.90***	–0.02	–0.02	–0.02	–0.02	**0.03**	0.00	0.02	–0.02	***–0.09***	***–0.08***	0.02	–0.02	0.00
frontal R	3.41	0.15	0.77	0.02	2.72	0.12	***–0.18***	***0.04***	*–0.07*	***0.92***	0.01	–0.02	0.00	**–0.04**	0.02	**0.03**	0.00	–0.02	***–0.07***	***–0.08***	0.01	–0.02	0.00
temporal L	2.60	0.11	0.72	0.03	2.07	0.09	***–0.23***	***–0.21***	*–0.09*	***0.86***	0.00	–0.03	***0.05***	–0.01	**0.04**	**0.03**	0.01	**–0.04**	–0.02	***–0.08***	0.02	–0.01	0.01
temporal R	2.63	0.13	0.71	0.03	2.10	0.10	***–0.24***	***–0.18***	*–0.10*	***0.85***	–0.01	–0.01	***0.08***	***–0.05***	**0.04**	**0.03**	–0.01	–0.03	0.00	***–0.08***	0.02	–0.01	0.02
parietal L	2.58	0.12	0.73	0.03	2.06	0.09	***–0.15***	***–0.24***	*–0.12*	***0.85***	0.00	–0.03	***–0.16***	**–0.04**	0.03	–0.02	0.00	0.00	0.00	***–0.05***	0.00	–0.01	0.00
parietal R	2.46	0.12	0.76	0.02	1.93	0.10	***–0.19***	***–0.27***	*–0.13*	***0.89***	0.00	**–0.06**	***–0.17***	***–0.06***	**0.04**	0.00	0.01	–0.01	**0.05**	***–0.05***	–0.01	0.00	–0.01
occipital L	1.85	0.08	0.43	0.04	1.47	0.07	***–0.23***	–0.03	–0.07	***0.66***	0.00	**–0.07**	***–0.16***	**–0.06**	**0.05**	0.01	0.05	0.00	**0.07**	–0.01	0.04	–0.01	**–0.04**
occipital R	1.78	0.07	0.46	0.04	1.43	0.06	***–0.27***	***–0.08***	*–0.09*	***0.69***	0.01	**–0.08**	***–0.15***	**–0.06**	0.03	**0.04**	**0.07**	–0.02	0.05	–0.01	**0.04**	–0.02	**–0.03**
cingulate L	0.72	0.03	0.58	0.03	0.57	0.02	***–0.15***	***0.06***	–0.01	***0.77***	0.00	–0.01	***0.08***	***–0.10***	**0.04**	0.00	–0.01	0.00	0.01	***–0.10***	0.01	0.00	0.00
cingulate R	0.68	0.03	0.51	0.04	0.54	0.02	***–0.12***	0.02	*–0.10*	***0.78***	–0.02	–0.02	***0.15***	***–0.11***	***0.11***	**–0.04**	–0.01	0.00	–0.01	***–0.15***	0.01	–0.01	–0.01
insular L	0.42	0.02	0.53	0.04	0.33	0.02	***–0.15***	–0.03	0.01	***0.71***	–0.01	–0.02	***–0.12***	–0.03	0.02	***0.07***	0.00	0.02	0.03	***–0.06***	0.01	0.01	–0.01
insular R	0.44	0.02	0.55	0.04	0.35	0.01	***–0.17***	***–0.09***	0.02	***0.67***	0.03	0.02	***–0.09***	**–0.06**	0.00	***0.07***	0.00	0.00	0.00	–0.04	0.02	0.00	0.00
Subcortical gray matter	2.52	0.12	0.69	0.03	1.99	0.09	***–0.22***	***–0.12***	*–0.07*	***0.82***	0.01	–0.02	***–0.13***	**–0.05**	–0.01	***0.05***	***0.08***	–0.02	**0.05**	0.01	0.00	0.00	0.01
thalamus L	0.41	0.02	0.58	0.04	0.33	0.01	***–0.27***	***–0.16***	–0.05	***0.70***	–0.01	0.01	***–0.12***	0.02	–0.02	***0.06***	**0.06**	**–0.04**	–0.01	0.00	–0.02	0.01	0.00
thalamus R	0.41	0.02	0.60	0.03	0.33	0.01	***–0.20***	***–0.15***	–0.04	***0.73***	0.01	0.01	***–0.13***	**–0.06**	**–0.06**	0.02	**0.04**	–0.02	0.04	0.01	–0.03	0.02	0.00
putamen L	0.39	0.02	0.45	0.04	0.31	0.01	***–0.18***	***–0.07***	0.02	***0.66***	0.02	–0.05	***–0.11***	**–0.06**	0.03	0.04	0.01	–0.02	**0.09**	–0.01	0.00	0.00	0.02
putamen R	0.34	0.02	0.47	0.04	0.27	0.01	***–0.12***	***–0.13***	–0.01	***0.66***	0.01	–0.03	***–0.19***	–0.05	0.01	0.04	**0.05**	–0.03	**0.08**	0.01	–0.01	0.00	0.00
hippocampus L	0.28	0.01	0.39	0.05	0.22	0.01	***–0.32***	***–0.15***	–0.07	***0.57***	0.00	–0.03	***–0.06***	–0.05	0.02	**0.06**	0.05	0.00	**0.08**	–0.02	**0.05**	0.02	–0.01
hippocampus R	0.30	0.01	0.49	0.04	0.24	0.01	***–0.24***	***–0.21***	–0.04	***0.64***	0.02	0.00	***–0.09***	–0.02	–0.01	**0.05**	0.03	–0.02	**0.06**	–0.01	0.02	–0.01	0.00
caudate L	0.34	0.01	0.28	0.04	0.27	0.01	0.02	***–0.09***	*–0.18*	***0.58***	–0.02	–0.01	***–0.13***	***–0.14***	–0.04	**0.06**	**0.08**	0.00	0.06	0.03	0.00	0.00	0.02
caudate R	0.38	0.02	0.30	0.05	0.31	0.01	***0.11***	***0.10***	*–0.10*	***0.53***	–0.02	0.01	***–0.14***	**–0.07**	–0.03	**0.05**	**0.06**	0.01	0.00	0.03	–0.02	0.01	0.01
amygdala L	0.14	0.01	0.38	0.04	0.11	0.01	***–0.19***	***–0.10***	0.05	***0.51***	–0.01	0.02	***–0.08***	0.00	0.01	0.00	**0.06**	–0.03	0.03	0.00	0.02	0.00	0.00
amygdala R	0.14	0.01	0.47	0.04	0.11	0.00	***–0.25***	***–0.11***	0.06	***0.57***	–0.01	0.02	***–0.08***	–0.04	0.03	**0.04**	0.04	**–0.05**	0.03	–0.02	0.00	0.00	0.01
pallidus L	0.17	0.01	0.45	0.05	0.13	0.01	***–0.17***	***–0.11***	*–0.11*	***0.72***	0.00	–0.05	–0.04	0.03	0.04	0.01	**0.05**	**–0.04**	**0.06**	0.00	0.01	0.00	0.03
pallidus R	0.16	0.01	0.38	0.05	0.13	0.01	***–0.21***	***–0.17***	*–0.11*	***0.64***	0.01	–0.04	–0.05	0.04	**0.07**	***0.07***	**0.07**	–0.04	0.03	0.01	–0.01	0.00	**0.04**
accumbens L	0.04	0.00	0.41	0.05	0.04	0.00	***–0.25***	***–0.09***	*–0.08*	***0.68***	0.02	**–0.08**	***0.07***	***0.10***	–0.04	**0.05**	***0.12***	0.01	**–0.08**	–0.02	0.02	0.00	0.00
accumbens R	0.05	0.00	0.35	0.05	0.04	0.00	***–0.17***	***0.07***	*–0.15*	***0.58***	–0.03	–0.02	***–0.06***	***–0.11***	***–0.22***	***0.08***	***0.17***	**–0.06**	–0.01	***0.08***	0.00	0.01	**0.04**
ventral diencephalon L	0.25	0.01	0.51	0.04	0.20	0.01	***–0.19***	0.03	0.03	***0.67***	–0.01	–0.03	–0.04	**–0.06**	–0.01	**0.05**	***0.09***	–0.01	0.04	0.01	0.01	0.00	–0.01
ventral diencephalon R	0.28	0.01	0.54	0.04	0.22	0.01	***–0.29***	0.00	–0.07	***0.71***	0.00	–0.01	***–0.05***	**–0.05**	0.00	0.03	**0.06**	–0.01	0.05	0.01	0.01	0.00	0.00
stem	1.54	0.07	0.48	0.05	1.24	0.06	***–0.08***	***–0.06***	–0.07	***0.67***	–0.01	–0.01	***–0.23***	–0.04	–0.02	0.03	***0.12***	**–0.05**	**0.08**	***0.07***	–0.03	0.00	–0.03
ventricle	0.15	0.01	0.38	0.05	0.12	0.00	***0.47***	***0.05***	*0.14*	***0.29***	–0.01	0.04	**0.05**	–0.03	0.00	–0.04	0.00	–0.03	–0.02	–0.02	0.01	0.01	–0.01

The values with p value <0.00125 are presented in bold and italic. The values with p value <0.05 are presented in bold. Kor, Korean; Cauc. Caucasian. L, left; R, right. MFS, magnetic field strength.

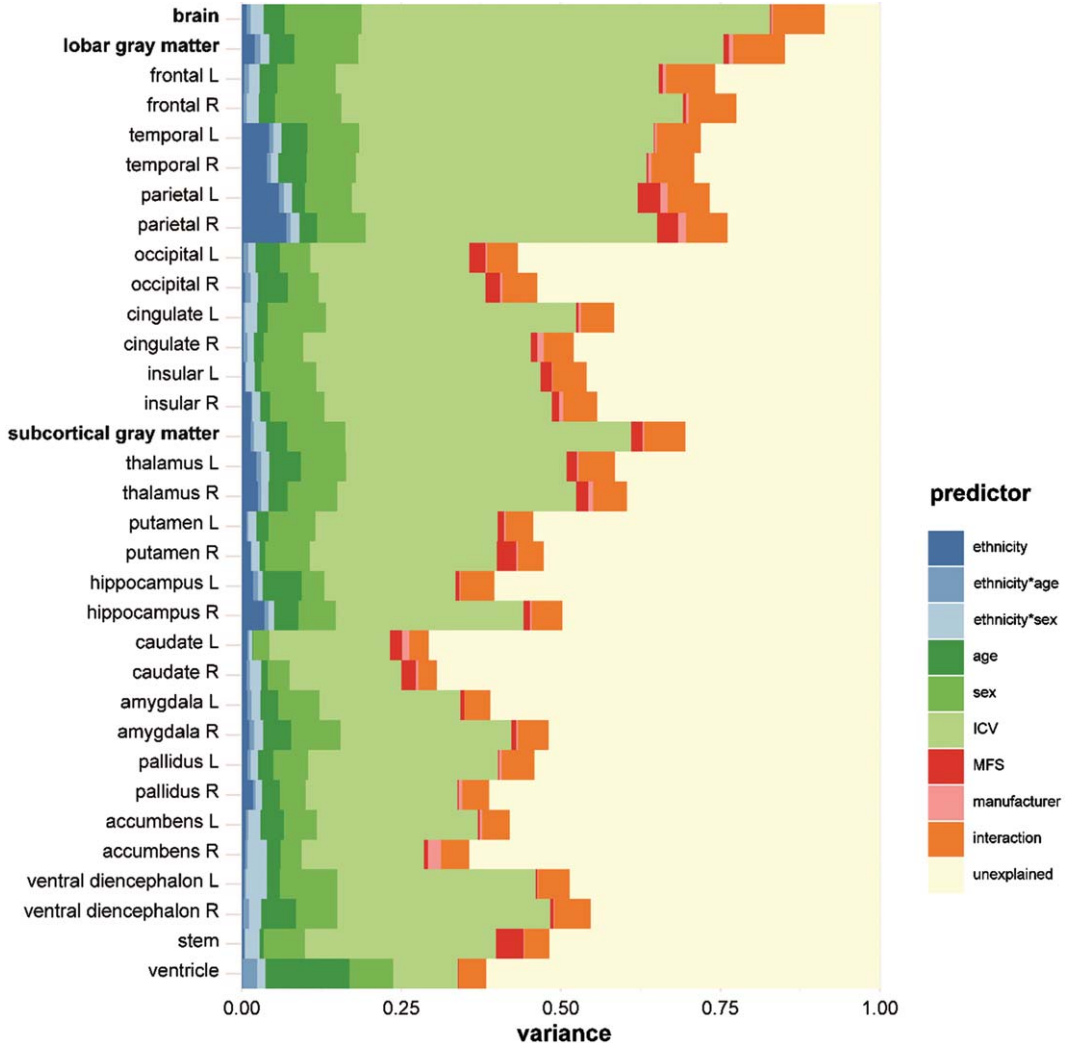

Fig. 3. Relative importance (R^2, proportion of the variance explained) of each predictive variable in the regression model for each regional volume. Ethnicity-related terms in blue collectively had a significant impact on brain volumes. The relative importance is calculated by averaging each predictor's explained proportion of the variance over all orderings of predictors. Interaction indicates the total of the proportions of variance explained by all the interaction terms except those pertaining to ethnicity.

was that all four types of Δz values for each region became less than –1 after correcting for ethnic disparities as indicated in Table 6. This resulted in the amygdalae, hippocampi, and the temporal cortices being chosen.

Figure 6 illustrated that after correcting for ethnic disparities, the distributions of z values for normal individuals became nearly indistinguishable between Koreans and Caucasians, in contrast to before correction. The pattern is also observed in the distribution of AD patients, though to a lesser degree than in the case of normal individuals. What's particularly noteworthy is the shift in the gap between the distributions of Korean AD patients and Caucasian normal controls. Before the correction, there was a significant degree of overlap between their distributions, which reduced after the correction. This reduction can be found in the columns labeled 'Kor-AD versus Cau-CN' of Table 6, as well as in Fig. 6.

For our concluding analysis, we performed diagnostic classification analysis, and examined the extent to which the correction for ethnic disparities enhances the performance of the AD classification models. We simply constructed logistic regression models using only the z values of six brain areas: bilateral amygdalae, hippocampi, and temporal lobes.

Table 3
Percentage of the variance explained by each predictor in models predicting lobar and subcortical regional volumes

	Ethnicity	Ethnicity*Age	Ethnicity*Sex	Age	Sex	ICV	MFS	Manufacturer	Interaction	Unexplained
brain	0.8	0.6	2.0	3.4	12.0	64.0	0.2	0.2	8.1	8.6
lobar gray matter	2.1	0.9	1.4	3.9	10.1	57.2	0.9	0.6	8.2	14.8
frontal L	0.4	0.7	1.6	2.7	9.2	50.6	0.6	0.5	7.7	25.8
frontal R	0.3	0.5	1.9	2.6	10.4	53.5	0.4	0.4	7.5	22.5
temporal L	4.3	0.7	1.2	4.1	8.2	46.1	0.2	0.4	6.9	28.0
temporal R	3.9	0.7	1.1	4.5	7.7	45.5	0.3	0.5	6.7	29.1
parietal L	5.9	0.7	1.2	2.0	7.5	44.7	3.6	1.1	6.6	26.6
parietal R	6.9	0.7	1.4	2.8	7.5	45.7	3.4	1.2	6.6	23.8
occipital L	0.2	0.8	1.1	3.8	4.8	24.9	2.5	0.3	4.9	56.7
occipital R	0.6	0.8	1.1	4.8	4.8	26.1	2.3	0.4	5.5	53.7
cingulate L	0.3	0.3	1.9	1.6	9.2	39.2	0.3	0.4	5.2	41.7
cingulate R	0.3	0.6	1.1	1.5	6.2	35.6	1.1	0.9	4.7	48.0
insular L	0.5	0.2	1.3	1.1	8.6	35.1	1.8	0.2	5.3	45.9
insular R	1.5	0.2	1.1	1.6	8.6	35.5	1.2	0.6	5.4	44.3
subcortical gray matter	1.5	0.5	1.9	3.3	9.1	44.7	1.8	0.2	6.4	30.5
thalamus L	2.3	0.8	1.2	5.0	7.0	34.6	1.5	0.3	5.7	41.5
thalamus R	2.5	0.6	1.1	3.0	7.8	37.5	1.9	0.7	5.2	39.7
putamen L	0.8	0.3	1.2	2.0	7.3	28.5	1.0	0.2	4.3	54.3
putamen R	1.4	0.2	1.2	0.9	7.0	29.3	3.0	0.2	4.1	52.6
hippocampus L	1.8	0.8	0.6	6.2	3.6	20.5	0.6	0.2	5.4	60.4
hippocampus R	3.6	0.6	0.9	3.8	5.9	29.4	1.0	0.3	4.8	49.8
caudate L	0.9	0.3	0.5	0.1	2.6	18.9	1.9	1.1	3.0	70.7
caudate R	0.7	0.6	1.7	1.0	3.4	17.6	2.3	0.3	2.9	69.4
amygdala L	0.9	0.7	1.4	2.8	6.4	22.1	0.7	0.1	4.0	61.1
amygdala R	1.2	0.8	1.4	4.4	7.7	26.8	0.8	0.3	4.8	51.9
pallidus L	0.9	0.5	1.1	2.4	5.4	29.8	0.2	0.3	5.2	54.1
pallidus R	1.8	0.4	0.9	2.9	4.1	23.8	0.2	0.5	4.2	61.2
accumbens L	0.6	0.4	1.9	3.6	5.2	25.2	0.3	0.4	4.3	58.0
accumbens R	0.6	0.3	3.0	2.2	3.2	19.2	0.6	2.1	4.4	64.4
ventral diencephalon L	0.4	0.3	3.3	2.1	9.0	31.1	0.3	0.1	4.9	48.6
ventral diencephalon R	0.2	0.9	1.9	5.6	6.5	33.4	0.4	0.1	5.7	45.3
stem	0.4	0.1	2.3	0.6	6.6	29.9	4.3	0.1	4.0	51.7
Ventricle	0.2	2.2	1.4	13.2	6.9	10.1	0.0	0.1	4.2	61.7

L, left; R, right; ICV, intracranial volume; MFS, magnetic field strength.

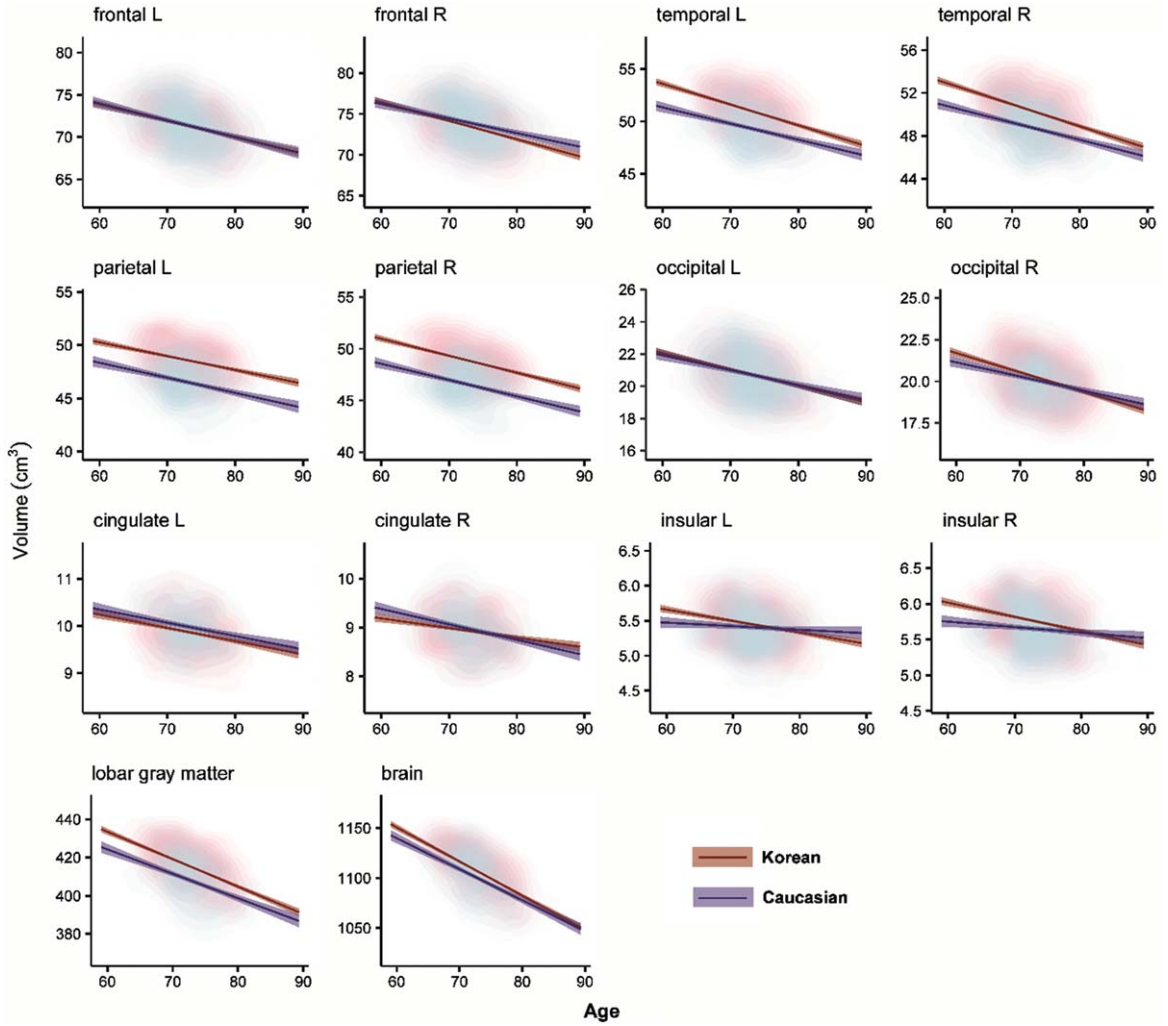

Fig. 4. Lobar volume changes with age in Korean (red) and Caucasian (blue) elderly people. This figure illustrates ethnic contrast on age effect in each model predicting lobar volumes in a massive sample of cognitively normal people aged 59–89. Each line denotes mean volume with 95% confidence intervals in the colored shade.

Figure 7 showed the classifiers' performances before (AUC = 0.81) and after correction for ethnic disparities (AUC = 0.85) in terms of the ROC. Following the correction, the classifier exhibited a significant enhancement compared to its pre-correction state with ΔAUC=0.04, $D = 4.18$, $p < 0.0001$, as determined by a bootstrap AUC comparison test.

DISCUSSION

General summary

The present study again highlights the importance of ethnicity as a predictor in the prediction model for normative brain volumes and the validity of multi-racial normative volumes of the brain to diagnose degenerative brain diseases. This research reproduced the key findings of our previous study that first presented multi-racial norms for lobar and subcortical volumes by using large samples restricted to people of old age [6]; moreover, in the present study, the self-developed software tool for brain volume measurement named Neuro I was used instead of FreeSurfer, so the model is now validated using two independent software programs for brain measurement.

This study found the brain areas most vulnerable to dementia for diagnostic application. The representative areas included the amygdala, hippocampus, and temporal lobe, and were sensitively different in vol-

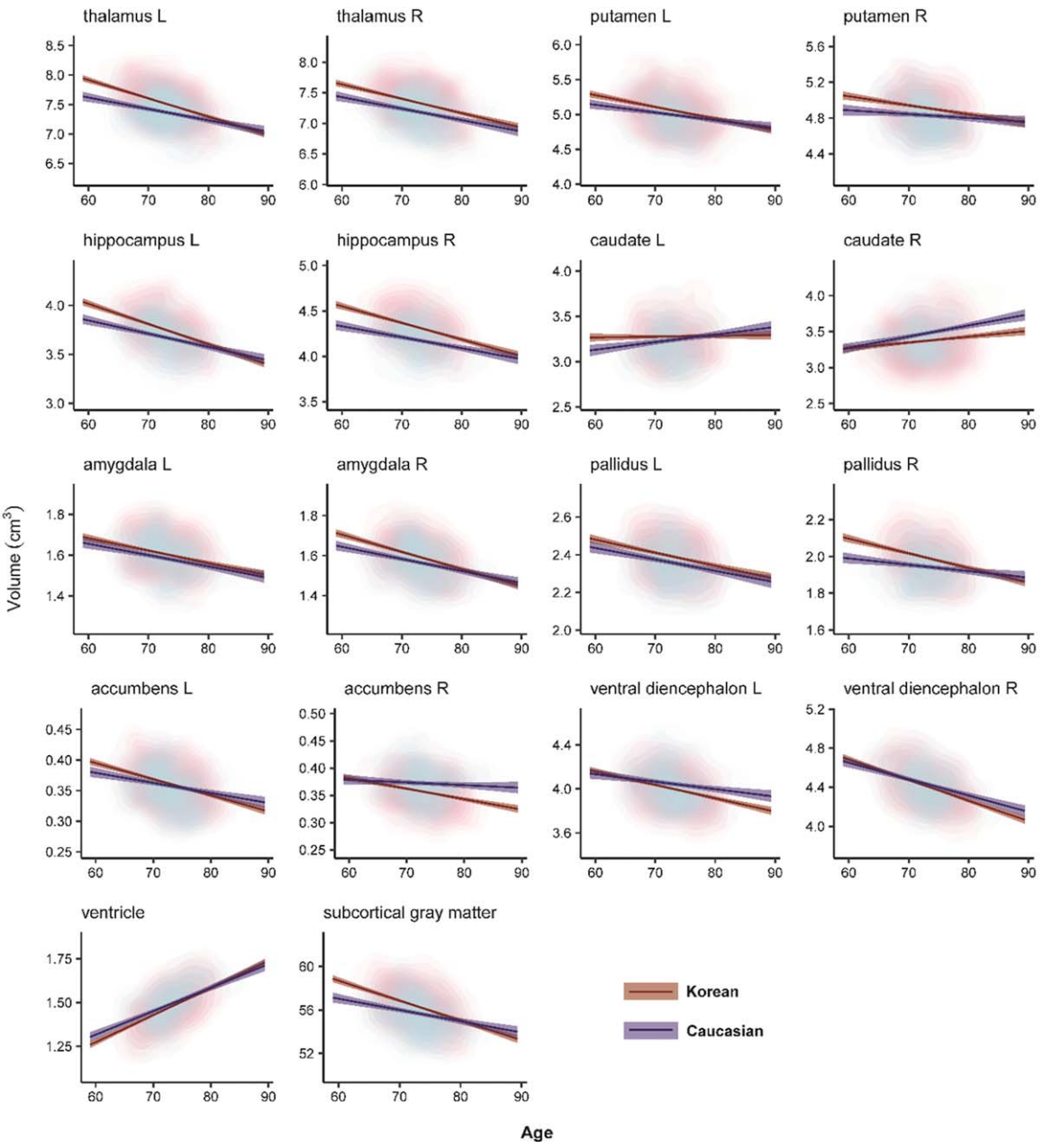

Fig. 5. Subcortical volume changes in Korean (red) and Caucasian (blue) elderly peoples. This figure illustrates age and ethnicity influence in each model predicting subcortical regional volumes in a large sample of cognitively healthy individuals aged 59–89. Shaded ribbons around each line denote 95% confidence intervals for the mean. The ventricular volume is $\log_{10}$ transformed.

ume according to ethnicity. The values for the areas corrected for racial disparities enhanced the diagnostic accuracy of the AD classifier models. These results were consistent with the results of our previous paper. Particularly, the results in Fig. 6 and Table 6 indicate that when medical practitioners analyze Korean AD patients' data, referring only to Caucasian norms may lead them to incorrect diagnoses. The doctors may be biased to diagnose patients as being within the normal range because of the extensive overlap in the distribution of brain regions, particularly the temporal cortices and the right hippocampus, between Caucasians without AD and Koreans with AD prior to ethnic disparity correction. Considering that the temporal lobes are situated laterally in the brain, and the Asian brain bulges laterally compared to

Table 4
Sample sizes of normal people and AD patients of Koreans and Caucasians

	Korean-CN		Korean-AD		Caucasian-CN		Caucasian-AD	
	M	±SD	M	±SD	M	±SD	M	±SD
n	214		214		214		214	
age	75.1	±5.8	75.1	±5.9	75.0	±5.6	75.8	±6.6
sex (male)	50.0%		50.0%		50.0%		50.0%	
education (y)	9.1	±5.0	7.9	±5.0	16.2	±2.7	15.0	±2.8
APOE ε4 carrier	24.3%		58.3%		29.0%		85.0%	
field strength (1.5T)	27.6%		29.9%		28.5%		39.3%	

the Caucasian brain [25], the temporal lobes may be influenced by genetic factors that affect both cranial shape and racial characteristics [26–28].

Review/Comparison of previous studies

Although this study and our previous paper were generally consistent in their conclusion, we identified minor differences. Before the ethnicity adjustment, the AD classifiers using Neuro I (AUC = 0.81) slightly outperformed the classifier using FreeSurfer (AUC = 0.78), but the ethnicity adjustment improved the performance of the classifier of FreeSurfer (ΔAUC=0.10. $D = 7.80$, $p < 0.001$) over that of the classifier of Neuro I (ΔAUC=0.04, $D = 4.18$, $p < 0.001$). The relatively weak effect of ethnicity on the performance of the classifier using Neuro I appears to be due to the ethnic effects that were less significant in most brain regions (for details, see Table 2 and Table 2 in Choi, et al. [6]).

Regardless of the brain volume measurement tool, Koreans were larger in most brain regions than Caucasians (Supplementary Table 1). Compared to FreeSurfer showing Koreans' largeness in all lobar structures, the use of Neuro I weakened the ethnic effects. Furthermore, Neuro I reversed the sign of the ethnic effects on the right frontal lobe and the left cingulate cortex. In subcortical structures, the use of Neuro I and FreeSurfer in both cases led to the conclusion that Koreans were larger in thalami, hippocampi, and amygdalae whereas they led to disagreement on conclusions as to whether a specific race was greater in putamina, left accumbens and left ventral diencephalon. In caudates, pallidi, and stem, it is difficult to conclude that the two tools led to different ethnic effects since the CIs of the two types of measures overlapped.

The data showed that the ethnic differences in brain volumes tended to be less substantial in most regions when using Neuro I than when using FreeSurfer (Supplementary Table 1). Except for a few regions, it is clear that using Neuro I largely reduced the ethnicity effect. The cause of this reduction is difficult to determine but the deep learning-based imaging processing of Neuro I does not rely upon standard template images and so may have contribute to reducing racial differences. Compared to Neuro I, FreeSurfer uses the brain template based on Caucasian brain images, so it is suboptimal for Asian brain analysis. Therefore, although the learning process was performed with Korean brain images, we are of the opinion that the deep learning-based method could be used successfully to increase the versatility of the image analysis for multiple ethnic groups.

In our investigation, the left caudate exhibited a unique pattern, showing no age-related alterations in normal aging. This observation was consistent across analyses conducted using both Neuro I and FreeSurfer data ($\beta_{age} = 0.02$ and –0.04, $p > 0.05$, respectively) [6]. This finding aligns with the results reported by Walhoved et al. [2], illustrating a stable or increased caudate volume in older age. Furthermore, Persson et al. [29] noted a larger caudate in AD patients compared to those with mild cognitive impairment or SCI. Table 6 also indicated marginally increased caudate volumes in AD patients compared to CN within each race, although the differences did not reach statistical significance (Δz=0.21 and 0.18, $p > 0.05$ for Koreans and Caucasians, respectively; cf. the 'Kor-AD versus Kor-CN' and 'Cau-AD versus Cau-CN' columns of the 'After ethnicity adjustment' panel). Our prior FreeSurfer results showed marginally and insignificantly decreased caudate volumes only in Caucasians (Δz=0.02 and –0.26, $p > 0.001$ for Koreans and Caucasians, respectively) [6]. We found a paper reporting a smaller caudate of fifteen AD patients, but the control group were not sex- and age-matched because they were selected from their staff and bystanders [30].

The left caudate atrophy in AD patients is reported to occur later and to be less severe than the right side [31, 32]. These studies were consistent with our previous results of FreeSurfer ($\Delta z_{left} > \Delta z_{right}$ for caudate), but the difference between Δz_{left} and

Table 5
Z-scores and the differences between the observed volumes and the predicted

	Before ethnicity adjustment						After ethnicity adjustment					
	Korean-CN			Caucasian-CN			Korean-CN			Caucasian-CN		
	Z	*t*	*p*	*z*	*t*	*p*	*z*	*t*	*p*	*z*	*t*	*p*
brain	0.19	0.63	0.530	–0.31	–0.99	0.323	0.12	0.39	0.695	–0.16	–0.50	0.617
lobar gray matter	0.18	0.83	0.410	–0.40	–1.82	0.070	0.03	0.15	0.879	–0.10	–0.42	0.678
frontal L	–0.01	–0.04	0.969	–0.07	–0.39	0.696	0.00	–0.01	0.996	–0.07	–0.42	0.674
frontal R	–0.04	–0.25	0.804	0.01	0.08	0.937	0.01	0.04	0.964	–0.09	–0.46	0.645
temporal L	0.15	1.03	0.304	**–0.48**	–3.08	0.002	–0.03	–0.22	0.825	–0.09	–0.55	0.579
temporal R	0.19	1.31	0.189	**–0.45**	–2.99	0.003	0.02	0.15	0.881	–0.09	–0.58	0.561
parietal L	0.26	1.79	0.073	***–0.56***	–3.83	0.000	0.02	0.15	0.884	–0.07	–0.42	0.677
parietal R	0.27	1.76	0.079	***–0.60***	–3.93	0.000	0.00	0.01	0.989	–0.03	–0.19	0.846
occipital L	0.09	0.81	0.416	0.03	0.28	0.777	0.10	0.89	0.377	0.03	0.28	0.778
occipital R	0.12	1.07	0.285	–0.03	–0.26	0.793	0.12	1.04	0.300	0.01	0.09	0.929
cingulate L	0.01	0.06	0.956	0.07	0.54	0.586	0.05	0.43	0.666	–0.03	–0.22	0.823
cingulate R	0.02	0.14	0.892	0.04	0.30	0.766	0.02	0.16	0.877	0.02	0.14	0.885
insular L	0.04	0.29	0.770	–0.08	–0.62	0.537	0.03	0.23	0.816	–0.05	–0.36	0.719
insular R	0.12	1.02	0.307	–0.14	–1.13	0.259	0.07	0.57	0.569	–0.01	–0.06	0.953
subcortical gray matter	0.10	0.70	0.484	–0.19	–1.33	0.185	0.06	0.44	0.663	–0.07	–0.46	0.645
thalamus L	0.11	0.93	0.352	**–0.29**	–2.32	0.021	0.04	0.30	0.762	–0.09	–0.74	0.461
thalamus R	0.15	1.23	0.220	**–0.29**	–2.27	0.024	0.06	0.45	0.651	–0.07	–0.53	0.595
putamen L	0.06	0.59	0.558	–0.13	–1.21	0.226	0.02	0.21	0.831	–0.04	–0.34	0.731
putamen R	0.11	1.02	0.309	–0.12	–1.14	0.257	0.06	0.52	0.603	0.02	0.16	0.874
hippocampus L	0.13	1.37	0.171	–0.15	–1.53	0.128	0.08	0.76	0.448	0.00	0.00	0.998
hippocampus R	0.18	1.73	0.084	**–0.34**	–3.01	0.003	0.06	0.58	0.566	–0.06	–0.54	0.587
caudate L	0.07	0.78	0.439	–0.09	–1.01	0.314	0.06	0.69	0.493	–0.04	–0.43	0.666
caudate R	–0.04	–0.50	0.619	0.15	1.77	0.078	0.07	0.77	0.439	–0.05	–0.58	0.560
amygdala L	0.08	0.79	0.432	–0.08	–0.80	0.422	0.04	0.41	0.680	0.01	0.08	0.938
amygdala R	0.15	1.36	0.174	–0.11	–0.95	0.344	0.11	0.97	0.331	0.00	0.03	0.974
pallidus L	0.07	0.67	0.503	–0.13	–1.19	0.234	0.02	0.17	0.865	0.00	–0.02	0.981
pallidus R	0.11	1.21	0.227	–0.09	–1.00	0.317	0.05	0.55	0.583	0.07	0.70	0.484
accumbens L	0.04	0.41	0.679	–0.13	–1.13	0.260	0.05	0.54	0.592	–0.11	–0.94	0.350
accumbens R	**–0.19**	–2.22	0.027	0.16	1.56	0.121	–0.04	–0.47	0.636	–0.10	–0.88	0.381
ventral diencephalon L	–0.09	–0.84	0.402	0.17	1.41	0.159	0.00	–0.02	0.981	0.02	0.17	0.868
ventral diencephalon R	–0.03	–0.24	0.813	0.06	0.52	0.602	0.02	0.18	0.856	–0.01	–0.07	0.943
stem	–0.05	–0.49	0.626	0.00	–0.02	0.981	–0.02	–0.19	0.847	–0.02	–0.21	0.831
Ventricle	0.00	–0.02	0.984	0.13	1.37	0.170	0.02	0.22	0.825	0.08	0.80	0.424

The values with p value < 0.00125 are presented in bold and italic. The values with p value < 0.05 are presented in bold. L, left; R, right; ICV, intracranial volume; MFS, magnetic field strength; Kor, Korean; Cau, Caucasian; AD, AD patients; CN, normal controls.

Table 6
Z-score differences between AD patients and controls before/after ethnicity adjustment

	Before ethnicity adjustment												After ethnicity adjustment											
	Kor-AD vs. Kor-CN			Cau-AD vs. Kor-CN			Kor-AD vs. Cau-CN			Cau-AD vs. Cau-CN			Kor-AD vs. Kor-CN			Cau-AD vs. Kor-CN			Kor-AD vs. Cau-CN			Cau-AD vs. Cau-CN		
	Δz	t	p	Δz	t	p	Δz	t	p	Δz	t	p	Δz	t	p	Δz	t	p	Δz	t	p	Δz	t	p
brain	***–1.13***	–11.40	0.000	***–1.60***	–13.60	0.000	***–0.63***	–5.81	0.000	***–1.10***	–8.74	0.000	***–1.14***	–11.36	0.000	***–1.42***	–12.16	0.000	***–0.86***	–7.85	0.000	***–1.15***	–9.16	0.000
lobar gray matter	***–1.02***	–10.22	0.000	***–1.75***	–16.07	0.000	***–0.43***	–3.97	0.000	***–1.17***	–9.89	0.000	***–1.05***	–10.26	0.000	***–1.42***	–12.66	0.000	***–0.92***	–8.24	0.000	***–1.29***	–10.67	0.000
frontal L	***–0.50***	–5.19	0.000	***–0.59***	–5.56	0.000	***–0.44***	–4.31	0.000	***–0.53***	–4.78	0.000	***–0.49***	–5.18	0.000	***–0.60***	–5.65	0.000	***–0.42***	–4.20	0.000	***–0.53***	–4.76	0.000
frontal R	***–0.40***	–4.32	0.000	***–0.39***	–3.73	0.000	***–0.46***	–4.61	0.000	***–0.45***	–4.05	0.000	***–0.40***	–4.31	0.000	***–0.52***	–5.09	0.000	**–0.30**	–3.07	0.002	***–0.43***	–3.95	0.000
temporal L	***–1.33***	–11.44	0.000	***–2.28***	–20.01	0.000	***–0.70***	–5.96	0.000	***–1.65***	–14.32	0.000	***–1.41***	–11.45	0.000	***–1.90***	–16.00	0.000	***–1.35***	–10.98	0.000	***–1.85***	–15.51	0.000
temporal R	***–1.07***	–9.54	0.000	***–2.15***	–18.38	0.000	***–0.43***	–3.80	0.000	***–1.51***	–12.91	0.000	***–1.12***	–9.58	0.000	***–1.79***	–14.89	0.000	***–1.01***	–8.73	0.000	***–1.67***	–14.13	0.000
parietal L	***–0.65***	–6.60	0.000	***–1.50***	–13.63	0.000	0.18	1.68	0.094	***–0.68***	–5.80	0.000	***–0.71***	–6.70	0.000	***–0.94***	–7.96	0.000	***–0.62***	–5.57	0.000	***–0.86***	–6.92	0.000
parietal R	***–0.52***	–5.51	0.000	***–1.51***	–13.57	0.000	***0.35***	3.48	0.001	***–0.64***	–5.49	0.000	***–0.59***	–5.65	0.000	***–0.89***	–7.25	0.000	***–0.55***	–5.10	0.000	***–0.86***	–6.77	0.000
occipital L	**–0.26**	–2.61	0.009	**–0.25**	–2.29	0.022	–0.20	–1.95	0.052	–0.19	–1.71	0.089	**–0.26**	–2.61	0.009	**–0.27**	–2.41	0.016	–0.19	–1.88	0.061	–0.20	–1.76	0.079
occipital R	***–0.38***	–3.81	0.000	**–0.29**	–2.80	0.005	**–0.23**	–2.22	0.027	–0.14	–1.32	0.186	***–0.38***	–3.81	0.000	**–0.27**	–2.62	0.009	**–0.27**	–2.66	0.008	–0.17	–1.55	0.122
cingulate L	***–0.51***	–5.44	0.000	***–0.50***	–5.45	0.000	***–0.58***	–5.81	0.000	***–0.57***	–5.82	0.000	***–0.51***	–5.43	0.000	***–0.63***	–6.77	0.000	***–0.43***	–4.34	0.000	***–0.54***	–5.58	0.000
cingulate R	***–0.44***	–4.33	0.000	***–0.57***	–5.58	0.000	***–0.46***	–4.46	0.000	***–0.60***	–5.69	0.000	***–0.43***	–4.32	0.000	***–0.58***	–5.61	0.000	***–0.43***	–4.24	0.000	***–0.58***	–5.50	0.000
insular L	***–0.69***	–6.91	0.000	***–0.70***	–6.23	0.000	***–0.57***	–5.61	0.000	***–0.58***	–5.09	0.000	***–0.69***	–6.92	0.000	***–0.68***	–6.07	0.000	***–0.62***	–6.03	0.000	***–0.61***	–5.31	0.000
insular R	***–0.63***	–6.16	0.000	***–0.72***	–6.57	0.000	***–0.37***	–3.62	0.000	***–0.45***	–4.17	0.000	***–0.64***	–6.18	0.000	***–0.58***	–5.29	0.000	***–0.56***	–5.48	0.000	***–0.50***	–4.61	0.000
subcortical gray matter	***–0.82***	–8.60	0.000	***–1.18***	–12.87	0.000	***–0.53***	–5.33	0.000	***–0.88***	–9.29	0.000	***–0.84***	–8.55	0.000	***–1.08***	–11.58	0.000	***–0.70***	–7.01	0.000	***–0.95***	–9.87	0.000
thalamus L	***–0.57***	–6.15	0.000	***–0.80***	–8.65	0.000	–0.17	–1.66	0.098	***–0.40***	–3.95	0.000	***–0.58***	–6.14	0.000	***–0.60***	–6.42	0.000	***–0.45***	–4.39	0.000	***–0.47***	–4.63	0.000
thalamus R	***–0.41***	–4.49	0.000	***–0.58***	–6.36	0.000	0.03	0.35	0.724	–0.13	–1.37	0.172	***–0.42***	–4.51	0.000	***–0.33***	–3.54	0.000	**–0.29**	–2.92	0.004	**–0.20**	–2.01	0.045
putamen L	***–0.47***	–4.79	0.000	***–0.75***	–7.57	0.000	**–0.29**	–2.87	0.004	***–0.56***	–5.62	0.000	***–0.48***	–4.81	0.000	***–0.65***	–6.54	0.000	***–0.42***	–4.20	0.000	***–0.59***	–5.92	0.000
putamen R	***–0.33***	–3.29	0.001	***–0.67***	–6.50	0.000	–0.09	–0.94	0.348	***–0.43***	–4.22	0.000	***–0.33***	–3.31	0.001	***–0.52***	–5.01	0.000	**–0.29**	–2.91	0.004	***–0.48***	–4.64	0.000
hippocampus L	***–1.67***	–13.58	0.000	***–2.20***	–19.38	0.000	***–1.38***	–11.22	0.000	***–1.91***	–16.82	0.000	***–1.69***	–13.50	0.000	***–2.06***	–18.03	0.000	***–1.61***	–12.89	0.000	***–1.99***	–17.35	0.000
hippocampus R	***–1.37***	–11.90	0.000	***–2.09***	–18.33	0.000	***–0.85***	–7.04	0.000	***–1.57***	–13.15	0.000	***–1.41***	–11.85	0.000	***–1.82***	–15.62	0.000	***–1.28***	–10.35	0.000	***–1.69***	–13.91	0.000
caudate L	0.21	1.91	0.057	0.06	0.57	0.571	**0.37**	3.20	0.001	**0.21**	2.07	0.039	0.21	1.90	0.058	0.08	0.86	0.393	**0.31**	2.70	0.007	0.18	1.79	0.075
caudate R	***0.45***	4.11	0.000	***0.56***	5.52	0.000	**0.26**	2.29	0.022	***0.36***	3.52	0.000	***0.46***	4.12	0.000	**0.28**	2.72	0.007	***0.58***	5.15	0.000	***0.40***	3.85	0.000
amygdala L	***–1.52***	–11.54	0.000	***–2.15***	–19.27	0.000	***–1.36***	–10.12	0.000	***–1.99***	–17.36	0.000	***–1.52***	–11.54	0.000	***–2.05***	–18.40	0.000	***–1.49***	–11.10	0.000	***–2.02***	–17.67	0.000
amygdala R	***–1.53***	–12.60	0.000	***–2.27***	–20.80	0.000	***–1.27***	–10.47	0.000	***–2.01***	–18.43	0.000	***–1.54***	–12.56	0.000	***–2.17***	–19.76	0.000	***–1.43***	–11.73	0.000	***–2.06***	–18.85	0.000
pallidus L	**–0.30**	–3.12	0.002	***–0.38***	–3.73	0.000	–0.10	–1.08	0.281	–0.19	–1.82	0.070	**–0.30**	–3.14	0.002	**–0.24**	–2.34	0.020	**–0.28**	–2.92	0.004	**–0.22**	–2.14	0.033
pallidus R	***–0.37***	–3.86	0.000	***–0.43***	–4.38	0.000	–0.16	–1.73	0.085	**–0.23**	–2.33	0.020	***–0.38***	–3.89	0.000	**–0.27**	–2.69	0.007	***–0.39***	–4.18	0.000	**–0.28**	–2.93	0.004
accumbens L	***–0.51***	–4.99	0.000	***–0.42***	–4.12	0.000	***–0.35***	–3.25	0.001	**–0.26**	–2.41	0.016	***–0.51***	–4.97	0.000	***–0.44***	–4.29	0.000	***–0.35***	–3.33	0.001	**–0.28**	–2.66	0.008
accumbens R	***–0.32***	–3.36	0.001	0.18	1.77	0.077	***–0.67***	–6.61	0.000	–0.17	–1.55	0.122	***–0.32***	–3.35	0.001	–0.19	–1.86	0.064	**–0.27**	–2.65	0.008	–0.14	–1.28	0.200
ventral diencephalon L	**–0.26**	–2.85	0.005	–0.05	–0.55	0.585	***–0.52***	–5.35	0.000	**–0.31**	–3.19	0.002	**–0.26**	–2.84	0.005	**–0.27**	–3.00	0.003	**–0.28**	–2.91	0.004	**–0.30**	–3.07	0.002
ventral diencephalon R	***–0.49***	–5.67	0.000	***–0.36***	–4.35	0.000	***–0.58***	–6.10	0.000	***–0.45***	–4.90	0.000	***–0.49***	–5.66	0.000	***–0.48***	–5.81	0.000	***–0.46***	–4.84	0.000	***–0.45***	–4.91	0.000
stem	–0.11	–1.22	0.222	–0.05	–0.54	0.592	–0.16	–1.68	0.093	–0.10	–1.00	0.317	–0.11	–1.22	0.225	–0.12	–1.20	0.232	–0.11	–1.13	0.257	–0.11	–1.12	0.263
ventricle	***0.85***	9.23	0.000	***1.00***	10.25	0.000	***0.72***	7.36	0.000	***0.87***	8.44	0.000	***0.85***	9.20	0.000	***0.94***	9.72	0.000	***0.80***	8.14	0.000	***0.89***	8.69	0.000

The values with p value < 0.00125 are presented in bold and italic. The values with p value < 0.05 are presented in bold. L, left; R, right; Kor, Korean; Cau, Caucasian; AD, AD patients; CN, normal controls.

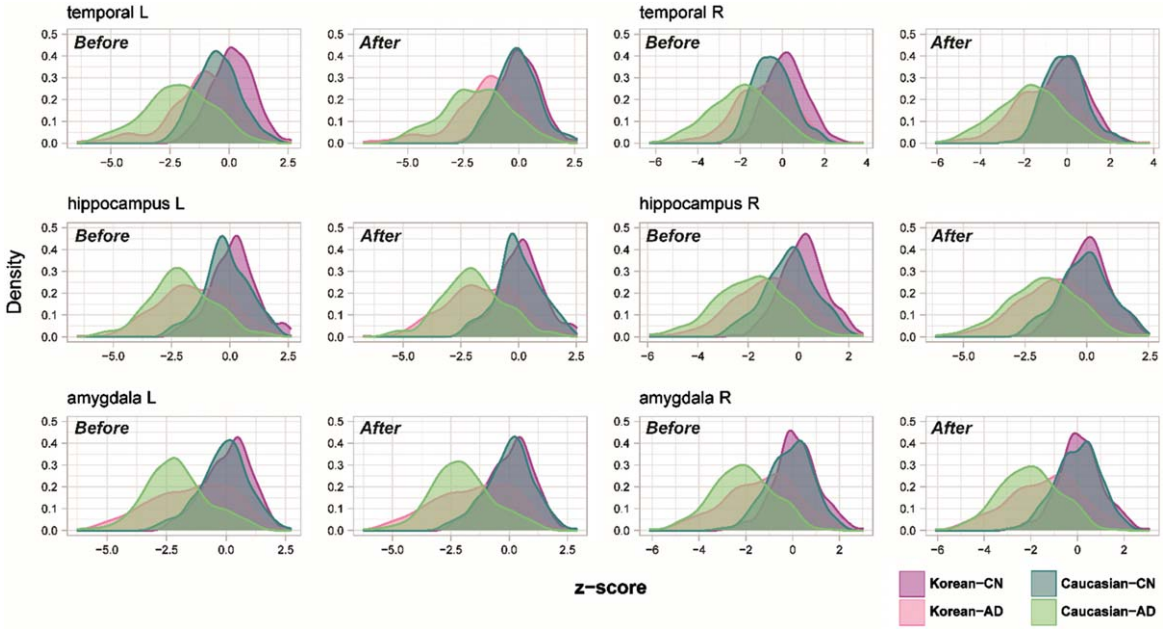

Fig. 6. Examples of z-score distributions of Alzheimer's diseases (AD) patients and normal controls (CN) before/after adjustment for ethnic differences. Before the adjustment, the z-score distributions of each diagnosis group were less overlapping between Koreans and Caucasians and then more overlapping after the adjustment.

Δz_{right} is too marginal to be statistically significant. In the case of Neuro I, both left and right caudates were not atrophied in AD patients. The caudate is anatomically wired to various brain regions and plays a crucial role in learning and memory. Specifically, studies indicate that the caudate volume is correlated to language proficiency [33]; and a stimulation to the caudate may improve learning and memory [34]. As individuals age, fluid cognitive abilities such as processing speed and executive functions tend to decline, whereas crystallized cognitive abilities like associative learning, knowledge, and comprehension continue to increase [35, 36]. Notably, the caudate nucleus appears to be involved in crystallized abilities, particularly in functions related to language and emotional aspects. Consequently, the left caudate nucleus is speculated to experience relatively less atrophy compared to other brain regions, suggesting that the caudate may be resilient to aging, and even serve as a compensatory mechanism [31, 37].

Neuro I and FreeSurfer originate from entirely different technical underpinnings. Neuro I employs a two-deep learning model pipeline for sequential brain tissue segmentation and ROI parcellation. The 3D CNN-based deep learning model was trained on a dataset comprising 778 cognitively normal Koreans,

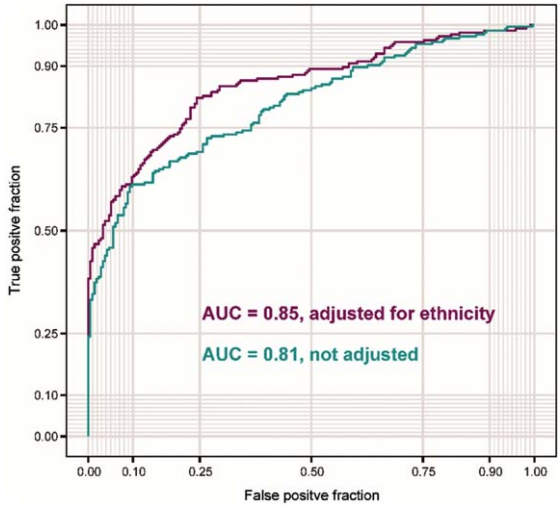

Fig. 7. Performance of the classifiers of Korean patients (AD) from Caucasian normal controls (CN) using z-scores of bilateral temporal cortices, hippocampi, and amygdalae before/after adjustment for ethnic differences.

focusing on precise brain tissue extraction and generating 109 ROIs [38]. On the contrary, FreeSurfer is grounded in conventional algorithms that have been developed and amassed over several decades, which incorporate the removal of non-brain tissue

using a hybrid watershed/surface deformation procedure [39], tessellation of the gray matter white matter boundary [40], registration to a spherical atlas which is based on individual cortical folding patterns to match cortical geometry across subjects [41], parcellation of the cerebral cortex into units with respect to gyral and sulcal structure [42], and so on in its segmentation and parcellation steps [43]. Despite its extensive technical heritage, FreeSurfer yielded more jagged and less smooth boundaries in parcellation of AD-vulnerable brain regions whereas Neuro I generated smoother and more well-defined boundaries [38]. Recently, deep-learning-based segmentation techniques have been widely used in various fields. Since deep learning techniques utilize feature information that previously could not be observed by humans, the techniques are expected to enable more accurate segmentation and parcellation than conventional methods.

Limitations

Because this study followed the methodology of our previous study, it also shared the limitations due to multi-study data analyses and other methodological features (for a more in-depth discussion, see our previous paper [6]). Additionally, as Choi et al. [6] mentioned, race or ethnicity is determined by both environmental and genetic factors, which makes it difficult to draw strong conclusions. The primary aim of our research is not to identify specific brain regions on which solely the genetic components of ethnicity have an impact, but rather to establish normative ethnic standards for brain volume and formulate strategies to minimize the current lack of compatibility between these standards.

Conclusions

The present study validated a regression model which incorporates an individual's ethnicity as variable for estimating brain volumes in older adults, which are used for diagnosis of neurodegenerative diseases. The validity of this model was established through the use of both a self-developed quantitative brain measurement software (Neuro I) and a widely-used standard tool (FreeSurfer). The results demonstrate that the z-scores derived from this model are effective for the diagnosis of AD regardless of the measurement tool employed. Our results provide valuable insights into the diagnostic processes of neurodegenerative diseases in multiethnic populations.

AUTHOR CONTRIBUTIONS

Yu Yong Choi (Formal analysis; Writing – original draft; imaging analysis); Jang Jae Lee (Formal analysis); Jan te Nijenhuis (Writing – original draft); Kyu Yeong Choi (Formal analysis); Jongseong Park (Software); Jongmyoung Ok (Software); Il Han Choo (interpreting the neuropsychological results); Hoo Won Kim (interviewing and examining the patients/participants and read the brain; MRIs); Min-Kyung Song (interpreting the neuropsychological results); Seong-Min Choi (interviewing and examining the patients/participants and read the brain MRIs); Soo Hyun Cho (interviewing and examining the patients/participants and read the brain MRIs); Youngshik Choe (interpreting the neuropsychological results); Byeong C. Kim (Conceptualization; Supervision; Writing – original draft; interviewing and examining the patients/participants and read the brain MRIs); Kun Ho Lee (Conceptualization; Supervision; Writing – original draft).

ACKNOWLEDGMENTS

The authors are grateful to the volunteers and their families in the GARD, ADNI, and OASIS studies. Some data used in the preparation of this article were obtained from the ADNI dataset (https://adni.loni.usc.edu) and the OASIS-3 dataset (https://www.oasis-brains.org/). Therefore, the investigators within ADNI and OASIS contributed to the design and implementation of their studies and/or provided data but did not participate in analysis or writing of this report. A complete listing of ADNI investigators can be found at: http://adni.loni.usc.edu/wp-content/uploads/how_to_apply/ ADNI_Acknowledgement_List.pdf. The information about OASIS-3 can be found at https://doi.org/ 10.1101/2019.12.13.19014902.

We wish to express our deep gratitude and pay tribute to Professor Dong-Hyun Kim, vice director of GARD Cohort Research Center, who made a great contribution to acquiring MRI data and conducting the research, and passed away at the age of 42 on June 11, 2014.

FUNDING

This research was supported by the Original Technology Research Program for Brain Science (2014M3C7A1046041 to KHL), and Bio

& Medical Technology Development Program (2016M3A9E9941914) of the National Research Foundation (NRF) funded by Ministry of Science and ICT, supported by KBRI basic research program through Korea Brain Research Institute funded by Ministry of Science and ICT (24-BR-03-05 to KHL, BCK. and YC), supported by the Korea National Institute of Health research project (2021-ER1007-01 to KHL), supported by the research grant from Chosun University, and supported by a grant of the Korea Health Technology R&D Project through the Korea Health Industry Development Institute (KHIDI), funded by the Ministry of Health & Welfare, Republic of Korea (HR20C0021 and HU20C0141 to BCK).

The Caucasian data were provided by OASIS (OASIS-3: Principal Investigators: T. Benzinger, D. Marcus, J. Morris; NIH P50 AG00561, P30 NS09857781, P01 AG026276, P01 AG003991, R01 AG043434, UL1 TR000448, R01 EB009352. The AV-45 doses were provided by Avid Radio-pharmaceuticals, a wholly owned subsidiary of Eli Lilly) and ADNI (NIH Grant U01 AG024904, DOD ADNI W81XWH-12-2-0012). The funding details of ADNI can be found at http://adni.loni.usc.edu/about/funding/.

CONFLICT OF INTEREST

YYC, JP, JO, and KHL were, or currently are, partly or fully employed by Neurozen Inc. The remaining authors declare that the research was conducted in the absence of any commercial or financial relationships that could be construed as a potential conflict of interest. The funders had no role in the design of the study; in the collection, analyses, or interpretation of data; in the writing of the manuscript; or in the decision to publish the results.

DATA AVAILABILITY

The datasets used in this study can be found in the online repositories: the ADNI dataset (https://adni.loni.usc.edu) and the OASIS-3 dataset (https://www.oasisbrains.org/). The GARD data supporting this study's findings are not openly available yet. Until we are ready to share the data publicly, the data could be available from the corresponding authors (BCK or KHL), upon reasonable request.

SUPPLEMENTARY MATERIAL

The supplementary material is available in the electronic version of this article: https://dx.doi.org/10.3233/JAD-231182.

REFERENCES

[1] Kruggel F (2006) MRI-based volumetry of head compartments: Normative values of healthy adults. *Neuroimage* **30**, 1-11.

[2] Walhovd KB, Westlye LT, Amlien I, Espeseth T, Reinvang I, Raz N, Agartz I, Salat DH, Greve DN, Fischl B, Dale AM, Fjell AM (2011) Consistent neuroanatomical age-related volume differences across multiple samples. *Neurobiol Aging* **32**, 916-932.

[3] Potvin O, Dieumegarde L, Duchesne S, Alzheimer's Disease Neuroimaging Initiative (2016) Normative data for subcortical regional volumes over the lifetime of the adult human brain. *Neuroimage* **137**, 9-20.

[4] Potvin O, Mouiha A, Dieumegarde L, Duchesne S, Alzheimer's Disease Neuroimaging Initiative (2016) FreeSurfer subcortical normative data. *Data Brief* **9**, 732-736.

[5] Kruggel F, Turner J, Muftuler LT, Alzheimer's Disease Neuroimaging Initiative (2010) Impact of scanner hardware and imaging protocol on image quality and compartment volume precision in the ADNI cohort. *Neuroimage* **49**, 2123-2133.

[6] Choi YY, Lee JJ, Choi KY, Choi U-S, Seo EH, Choo ILH, Kim H, Song M-K, Choi SM, Cho SH, Choe Y, Kim BC, Lee KH (2021) Multi-racial normative data for lobar and subcortical brain volumes in old age: Korean and Caucasian norms may be incompatible with each other. *Front Aging Neurosci* **13**, 675016.

[7] Beals KL, Smith CL, Dodd SM (1984) Brain size, cranial morphology, climate, and time machines. *Curr Anthropol* **25**, 301-330.

[8] William White H (1990) *Skull Shapes and the Map: Craniometric Analyses in the Dispersion of Modern Homo*, Peabody Museum Press, Cambridge, Massachusetts.

[9] Rushton JP (2000) *Race, evolution, and behavior: A life history perspective*, Charles Darwin Research Institute, Port Huron, MI.

[10] Ball R, Shu C, Xi P, Rioux M, Luximon Y, Molenbroek J (2010) A comparison between Chinese and Caucasian head shapes. *Appl Ergon* **41**, 832-839.

[11] Ledig C, Schuh A, Guerrero R, Heckemann RA, Rueckert D (2018) Structural brain imaging in Alzheimer's disease and mild cognitive impairment: Biomarker analysis and shared morphometry database. *Sci Rep* **8**, 11258.

[12] Resnick SM, Pham DL, Kraut MA, Zonderman AB, Davatzikos C (2003) Longitudinal magnetic resonance imaging studies of older adults: A shrinking brain. *J Neurosci* **23**, 3295-3301.

[13] Scahill RI, Frost C, Jenkins R, Whitwell JL, Rossor MN, Fox NC (2003) A longitudinal study of brain volume changes in normal aging using serial registered magnetic resonance imaging. *Arch Neurol* **60**, 989-994.

[14] Sowell ER, Peterson BS, Thompson PM, Welcome SE, Henkenius AL, Toga AW (2003) Mapping cortical change across the human life span. *Nat Neurosci* **6**, 309-315.

[15] He W, Goodkind D, Kowal P, Almasarweh IS, Giang TL, Islam MM, Lee S, Teerawichitchainan B, Tey NP (2022) Asia Aging: Demographic, Economic, and Health Transitions. *International Population Reports*, U.S. Census Bureau, Washington, DC. Report Number: P95/22-1

[16] Tustison NJ, Avants BB, Cook PA, Zheng Y, Egan A, Yushkevich PA, Gee JC (2010) N4ITK: Improved N3 bias correction. *IEEE Trans Med Imaging* **29**, 1310-1320.

[17] Çiçek Ö, Abdulkadir A, Lienkamp SS, Brox T, Ronneberger O (2016) 3D U-Net: Learning Dense Volumetric Segmentation from Sparse Annotation. In *Medical Image Computing and Computer-Assisted Intervention – MICCAI 2016*, Ourselin S, Joskowicz L, Sabuncu M, Unal G, Wells W, eds. Springer.

[18] Isensee F, Kickingereder P, Wick W, Bendszus M, Maier-Hein KH (2019) No New-Net. In *Brainlesion: Glioma, Multiple Sclerosis, Stroke and Traumatic Brain Injuries. BrainLes 2018*, Crimi A, Bakas S, Kuijf H, Keyvan F, Reyes M, van Walsum T, eds. Springer, Cham, pp. 234-244.

[19] Dahnke R, Yotter RA, Gaser C (2013) Cortical thickness and central surface estimation. *Neuroimage* **65**, 336-348.

[20] Folstein MF, Folstein SE, McHugh PR (1975) "Mini-mental state". A practical method for grading the cognitive state of patients for the clinician. *J Psychiatr Res* **12**, 189-198.

[21] Kang Y, Jang S, Na DL (2012) *Seoul Neuropsychological Screening Battery (SNSB)*, Human Brain Research & Consulting Co., Seoul.

[22] Morris JC (1993) The Clinical Dementia Rating (CDR): Current version and scoring rules. *Neurology* **43**, 2412-2414.

[23] Crawford JR, Garthwaite PH, Denham AK, Chelune GJ (2012) Using regression equations built from summary data in the psychological assessment of the individual case: Extension to multiple regression. *Psychol Assess* **24**, 801-814.

[24] Carpenter J, Bithell J (2000) Bootstrap confidence intervals: When, which, what? A practical guide for medical statisticians. *Stat Med* **19**, 1141-1164.

[25] Liang P, Shi L, Chen N, Luo Y, Wang X, Liu K, Mok VCT, Chu WCW, Wang D, Li K (2015) Construction of brain atlases based on a multi-center MRI dataset of 2020 Chinese adults. *Sci Rep* **5**, 18216.

[26] Chee MWL, Zheng H, Goh JOS, Park D, Sutton BP (2011) Brain structure in young and old East Asians and Westerners: Comparisons of structural volume and cortical thickness. *J Cogn Neurosci* **23**, 1065-1079.

[27] Tang Y, Zhao L, Lou Y, Shi Y, Fang R, Lin X, Liu S, Toga A (2018) Brain structure differences between Chinese and Caucasian cohorts: A comprehensive morphometry study. *Hum Brain Mapp* **39**, 2147-2155.

[28] Zilles K, Kawashima R, Dabringhaus A, Fukuda H, Schormann T (2001) Hemispheric shape of European and Japanese brains: 3-D MRI analysis of intersubject variability, ethnical, and gender differences. *Neuroimage* **13**, 262-271.

[29] Persson K, Bohbot VD, Bogdanovic N, Selbaek G, Braekhus A, Engedal K (2018) Finding of increased caudate nucleus in patients with Alzheimer's disease. *Acta Neurol Scand* **137**, 224-232.

[30] Jiji S, Smitha KA, Gupta AK, Pillai VP, Jayasree RS (2013) Segmentation and volumetric analysis of the caudate nucleus in Alzheimer's disease. *Eur J Radiol* **82**, 1525-1530.

[31] Cho H, Kim JH, Kim C, Ye BS, Kim HJ, Yoon CW, Noh Y, Kim GH, Kim YJ, Kim JH, Kim CH, Kang SJ, Chin J, Kim ST, Lee KH, Na DL, Seong JK, Seo SW (2014) Shape changes of the basal ganglia and thalamus in Alzheimer's disease: A three-year longitudinal study. *J Alzheimers Dis* **40**, 285-295.

[32] Madsen SK, Ho AJ, Hua X, Saharan PS, Toga AW, Jack CR, Jr., Weiner MW, Thompson PM, Alzheimer's Disease Neuroimaging Initiative (2010) 3D maps localize caudate nucleus atrophy in 400 Alzheimer's disease, mild cognitive impairment, and healthy elderly subjects. *Neurobiol Aging* **31**, 1312-1325.

[33] Hervais-Adelman A, Egorova N, Golestani N (2018) Beyond bilingualism: Multilingual experience correlates with caudate volume. *Brain Struct Funct* **223**, 3495-3502.

[34] Bick SK, Patel SR, Katnani HA, Peled N, Widge A, Cash SS, Eskandar EN (2019) Caudate stimulation enhances learning. *Brain* **142**, 2930-2937.

[35] Craik FI, Bialystok E (2006) Cognition through the lifespan: Mechanisms of change. *Trends Cogn Sci* **10**, 131-138.

[36] Choi YY, Shamosh NA, Cho SH, DeYoung CG, Lee MJ, Lee JM, Kim SI, Cho ZH, Kim K, Gray JR, Lee KH (2008) Multiple bases of human intelligence revealed by cortical thickness and neural activation. *J Neurosci* **28**, 10323-10329.

[37] Bohbot VD, Del Balso D, Conrad K, Konishi K, Leyton M (2013) Caudate nucleus-dependent navigational strategies are associated with increased use of addictive drugs. *Hippocampus* **23**, 973-984.

[38] Moon CM, Lee YY, Hyeong KE, Yoon W, Baek BH, Heo SH, Shin SS, Kim SK (2023) Development and validation of deep learning-based automatic brain segmentation for East Asians: A comparison with Freesurfer. *Front Neurosci* **17**, 1157738.

[39] Segonne F, Dale AM, Busa E, Glessner M, Salat D, Hahn HK, Fischl B (2004) A hybrid approach to the skull stripping problem in MRI. *Neuroimage* **22**, 1060-1075.

[40] Segonne F, Pacheco J, Fischl B (2007) Geometrically accurate topology-correction of cortical surfaces using nonseparating loops. *IEEE Trans Med Imaging* **26**, 518-529.

[41] Fischl B, Sereno MI, Tootell RBH, Dale AM (1999) High-resolution intersubject averaging and a coordinate system for the cortical surface. *Hum Brain Mapp* **8**, 272-284.

[42] Fischl B, van der Kouwe A, Destrieux C, Halgren E, Ségonne F, Salat DH, Busa E, Seidman LJ, Goldstein J, Kennedy D, Caviness V, Makris N, Rosen B, Dale AM (2004) Automatically parcellating the human cerebral cortex. *Cereb Cortex* **14**, 11-22.

[43] Grimm O, Pohlack S, Cacciaglia R, Winkelmann T, Plichta MM, Demirakca T, Flor H (2015) Amygdalar and hippocampal volume: A comparison between manual segmentation, Freesurfer and VBM. *J Neurosci Methods* **253**, 254-261.